Molecular Dynamics Simulations and *in silico* Analysis of Supramolecular Self-assembled Structures

Corneliu Cojocaru, Andrei Neamtu, Tudor Vasiliu, Dragos Lucian Isac, and Mariana Pinteala

Abstract In this contribution, we summarize the results that we have attained throughout the implementation of the SupraChemLab project (running from 2015 to 2020). Herein, we have focused on molecular dynamics simulations and *in silico* analysis of the supra-molecular structures and systems (such as water channels, biomembranes, and polyplexes). Molecular dynamics simulations were performed using dedicated professional software packages, *i.e.* GROMACS and YASARA. Computational outcomes revealed valuable insights concerning the supra-molecular self-assembled systems.

Keywords Molecular dynamics · Force fields · Computational chemistry · Supramolecular chemistry · Artificial water channels · Polyplexes · Solute-solvent interactions

C. Cojocaru
Department of Inorganic Polymers, "Petru Poni" Institute of Macromolecular Chemistry, 700487 Iasi, Romania
e-mail: cojocaru.corneliu@icmpp.ro

A. Neamtu (✉)
Physiology Department, "Grigore T. Popa" University of Medicine and Pharmacy, Str. Universitatii nr. 16, 700115 Iasi, Romania
e-mail: andrei.neamtu@umfiasi.ro

T. Vasiliu · M. Pinteala
Centre of Advanced Research in Bionanoconjugates and Biopolymers, "Petru Poni" Institute of Macromolecular Chemistry, 700487 Iasi, Romania
e-mail: vasiliu.tudor@icmpp.ro

M. Pinteala
e-mail: pinteala@icmpp.ro

D. L. Isac
Department of Physical Chemistry of Polymers, "Petru Poni" Institute of Macromolecular Chemistry, 700487 Iasi, Romania
e-mail: isac.dragos@icmpp.ro

M. J. M. Abadie et al. (eds.), *New Trends in Macromolecular and Supramolecular Chemistry for Biological Applications*, https://doi.org/10.1007/978-3-030-57456-7_18

Abbreviations

AMC	*Azobenzene maleimide compound*
AQPs	Aquaporins
AWC	Artificial water channels
b-PEI	Branched poly(ethylene imine)
β-CD	B-cyclodextrin
cD_4^H	2,4,6,8-tetramethylcyclotetrasiloxane,
DFT	Density functional theory
DNA	Deoxyribonucleic acid
dsDNA	Double-stranded deoxyribonucleic acid
DOTA	1,4,7,10-tetraazacyclododecane-1,4,7,10-tetraacetic acid
HBA	Hydrogen bond acceptor
HBD	Hydrogen bond donor (HBD)
MD	Molecular dynamics
MM	Molecular mechanics
PEG	Polyethylene glycol
PEI	Poly(ethylene imine)
PLL	Poly(L-Lysine)
POPC	Phosphatidylcholine
RNA	Ribonucleic acid
QM	Quantum mechanics
TIP3P	Three-site water model of rigid geometry

1 Introduction: Molecular Mechanics and Dynamics in Brief

Computational chemistry represents an essential molecular modeling tool employed in modern chemistry and biochemistry. Molecular modeling is very important nowadays to detail the structures and dynamics of molecules, macromolecules and complexes. Generally, computational chemistry comprises two main parts: (1) quantum mechanics (QM), and (2) molecular mechanics (MM) (Jensen 2007; Lewars 2004). In quantum mechanics (QM), the smallest particles subjected to modeling (by Schrödinger equation) are electrons and nuclei. Hence, QM treats electrons explicitly and enables to explore the small and medium-sized molecules with electronic structure methods. By contrast, in molecular mechanics, the nuclei and electrons are not treated explicitly; they are lumped together and treated as unified atom-like particles. Consequently, the atom-like particle is commonly treated as a sphere (ball) having certain size, mass and assigned partial charge. Moreover, in MM the bonds between atoms are viewed as springs (harmonic oscillators). Assuming classical mechanical principles, the MM permits to model efficiently large molecular structures (with thousands of atoms and even more). According to MM theory, the interactions between

atoms are treated using potential functions. For instance, the mathematics of spring deformation (Hooke's Law) is employed to model the bonded interactions, *i.e.* the ability of bonds to stretch, bend and twist. Non-bonded interactions are assessed by considering the Van der Waals attraction, steric repulsion, as well as electrostatic attraction/repulsion between non-bonded atoms. Commonly, the Van der Waals interactions are modeled by using Lennard-Jones 12-6 potentials and considering a fixed cut-off (*i.e.*, a short-range interacting distance, typically of 8–10 Å). In turn, the long-range electrostatic interactions are calculated by Coulombic model and Ewald summation. The total potential energy (U) of a molecule can be expressed as the summation of energy contributions from bond stretching, angle bending, torsional motion (rotation) around the single bonds, and interactions between non-bonded atoms (Lewars 2004).:

$$U = \sum_{bonds} U_{stretch} + \sum_{angles} U_{bend} + \sum_{dihedrals} U_{torsion} + \sum_{pairs} U_{nonbond} \quad (1)$$

Each energy contribution term is detailed in the textbooks (Jensen 2007; Lewars 2004; MacKerell Jr 2001). The mathematical expression of the potential energy and associated parameters is known as a *force-field*. Therefore, the MM approaches are sometimes called *force-filed* methods (Jensen 2007; Lewars 2004). During the last decades, many different types of force-fields were developed. Some of them include additional energy terms in order to improve the accuracy of the mechanical model. The force-field parameters must be optimized for a particular set of potential energy functions. This procedure is known as force-field parametrization. The classical force-fields that handle molecules involving much elements of the periodic table are MM2, MM3, MM4, UFF, and Sybyl (Lewars 2004). For modeling of biological macromolecules (proteins, nucleic acids) other important force-fields are employed such as AMBER, CHARMM, GROMOS, OPLS, YASARA, NOVA, and YAMBER (Guvench and MacKerell 2008; Krieger et al. 2002; Krieger and Vriend 2015).

A versatile computational tool relying on force-filed approach is the *molecular dynamics* simulation approach. In fact, *molecular dynamics* (MD) is a technique that uses numerical integration of Newton's equation of motion ($F_i = m_i \ddot{r}_i$) to simulate the time evolution of atoms in the molecular and polymeric systems. For example, by using the Verlet integration (based on finite-difference technique) the evolution of the atomic position against time can be estimated as (Becker and Watanabe 2001):

$$\mathbf{r}_{(n+1)} = \mathbf{r}_n + \mathbf{v}_n \Delta t + 0.5(\mathbf{F}_n/m)\Delta t^2 \quad (2)$$

where, $\mathbf{r}_n$ indicate the particle position (vector of all atomic coordinates) at step n (at time t), and $\mathbf{r}_{n+1}$ indicates the position at the next step $n + 1$ (at time $t + \Delta t$), **m—**mass of involved particles; $\mathbf{v}_n$—velocity of particles and $\mathbf{F}_n$—force acting on particles at step n. The velocity at the next step ($n + 1$) can be roughly ascertained as $\mathbf{v}_{n+1} = (\mathbf{r}_{n+1} - \mathbf{r}_n)/2$. Note that the force, in this approach, is determined by the gradient of the potential energy function, as given by (Becker and Watanabe 2001):

$$\mathbf{F}_n = -\nabla U(\mathbf{r}_n) \tag{3}$$

It is worth mentioning that in the last decades more accurate numerical algorithms have been developed to solve the equations of motions (by adopting the same kind of reasoning). Generally, the MD simulation protocol consists of several main steps (Becker and Watanabe 2001), detailed in the following.

1. *Preparation of modeling system*: This step implies the model generation, preparation of the initial coordinates for the structures and assignment of initial velocities (e.g. by Maxwell-Boltzmann distribution). Likewise, this initial phase involves the adding of missing hydrogen atoms; defining the simulation cell/box; solvation of the molecular structures by adding explicit solvent molecules (like TIP3P for water); defining the cell boundaries like periodic-type or wall-type, etc. Moreover, the system relaxation is performed by minimization of the initial structure to diminish the local strain and then gradually heating-up the system to the desired temperature.
2. *Equilibration*: In this phase, a 'short-term' dynamic simulation is performed that lasts from tens of picoseconds (ps) to several hundred of ps. The purpose of equilibration phase is to verify that the simulation is stable and free of irregular fluctuations.
3. *Production*: After equilibration, the system is considered reliable for long-term dynamics simulations. In a MD simulation with no pressure control, the volume of the simulation cell is held fixed. Instead, at constant-pressure MD the volume of the system may fluctuate. Nowadays, the production runs take from several nanoseconds up to microsecond-scale (depending on the system size and computer power). Note that the typical time-step for integration of equations of motion is 1 or 2 fs (femtoseconds, 10^{-15} s). The generated trajectories in the production phase are stored for further analysis.
4. *Analysis*: The last phase is dedicated to the careful analysis of the resulting molecular dynamics trajectories that was stored as 'snapshots' taken at equal time intervals. In this phase the time-dependent plots are developed to understand the dynamics (averages and fluctuations) of the investigated system.

In summary, molecular dynamics (MD) simulation is essential for studying structures, interactions and dynamics of (macro)/molecular systems. Therefore, MD has been successfully applied in supra-molecular chemistry to assess many important aspects, such as (a) the dynamics of conformations, (b) dynamics of intermolecular interactions (protein-protein, protein-drug, protein-DNA), (c) functionality of water/ionic channels in biological membranes, (d) stability of receptor-ligand complexes and polyplexes, (e) solute-solvent interactions, and others. Molecular dynamics simulations can be carried out using special program packages developed for this purpose, such as GROMACS, NAMD/VMD, AMBER, YASARA, LAMMPS, SCIGRESS, and others.

2 Molecular Dynamics of Water Permeation Across DOTA-Based Artificial Channels

Transport of substances (e.g. water, ions) across biological membranes represents a fundamental process in all living cells. In this respect, the proteins embedded in the lipid bilayer membranes play a crucial role. Such proteins (acting as accessing gates and channels) constitute in fact the highly selective diffusive pathways that control the inflow and outflow of substances through cellular membranes. Nowadays, simulations on membrane proteins deal with water and ion channels, as well as various transporters (Khalili-Araghi et al. 2009). Aquaporins (AQPs) are special type of channel-proteins (embedded into the biological membranes), which have the function of fast water transport (Barboiu 2016); thereby facilitating the moving of water molecules between intracellular and extracellular environments. For biological processes it is of great importance to understand the dynamics of the transport through the confined space of protein channels. In the last years, the artificial water channels (AWC) have attracted much attention (Barboiu 2016; Murail et al. 2018). The development of AWC is aimed to mimic the high water permeability observed for biological systems such as AQPs, as well as their selectivity to reject ion permeation simultaneously. Recently, Murail and co-workers (Murail et al. 2018) showed (by using molecular dynamics) that the self-assembling alkylureidoethylimidazole compounds have formed imidazole-quartet channels (I-quartets) that can act as artificial water channels.

In this report, we assessed the self-assembling of DOTA molecules into a supramolecular aggregate aiming to be tested as the potential artificial water channel. Note that DOTA represents an organic compound (1,4,7,10-tetraazacyclododecane-1,4,7,10-tetraacetic acid), which is mainly used as a complexing agent (chelator). The investigations were done by molecular dynamics simulations, where phosphatidylcholine (POPC) was employed as the main lipid constituent of the simulated bio-membrane. Thus, we investigated the DOTA self-assembly in the phospholipid (POPC) membrane and the water permeation through this artificial channel. The analysis of self-assembling simulations (starting from fully random mixtures of DOTA/POPC/water/ions) revealed the formation of DOTA aggregates in phospholipid membrane environments. Computational results disclosed that DOTA molecules preferred to "stay together" but still, with no phase separation. Stacks of two DOTA molecules could be identified which seems to strongly interact as they move together as a whole (i.e. the central ring and the nearby -NH-CO- moieties of the adjacent molecules display collective motions). The central cycles were arranged in a parallel orientation and the inter-molecular interaction was strengthened by H-bonds formed between -N-H groups of one DOTA molecule and the -C = O group of the next molecule. This stable arrangement may favor formation of stacks composed of several DOTA molecules with a proper dimension to completely traverse the membrane from one face to the other. This could provide a pathway for water permeation. In order to study the stability of such assemblies and water passage along them we constructed stacks of 6 DOTA molecules and inserted them in the POPC-based membrane. The

number of DOTA molecules had been chosen on the basis of hydrophobic match between the POPC bilayer core and the stack height (we tried with 4–7 molecules). In order to determine the mechanism through which DOTA molecules create water channels in a lipid bilayer we stacked 6 DOTA molecules and inserted them in a lipid bilayer consisting of 130 POPC molecules using 'membed' algorithm from the GROMACS 5·1 software. This simulation is called 1DOTA in the following. The insertion led to the deletion of 8 POPC molecules to a final count of 122. The system was hydrated with 7027 water molecules. The main results of the above described simulations are illustrated in Figs. 1, 2, 3, giving the short explanations in the figure captions.

Thus, the computation results unveiled that the water permeation events occur basically at lateral positions from the central rings. And, the water wire, in this case, emerged as jumping effects of water molecules between the binding sites pinpointed in between the -N-H and -C = O moieties of the rings (Figs. 1, 2, 3).

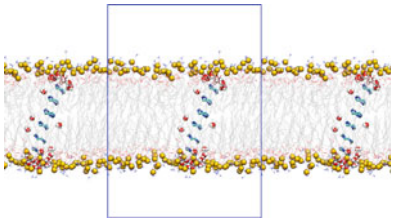

Fig. 1 Snapshot of the simulated system at the end of 1DOTA simulation (1 μs). The alkyl tails of DOTA molecules were removed for clarity. Some water molecules can be seen in the vicinity of the central ring of DOTA; phosphorus atoms of POPC have been represented as vdw spheres in yellow

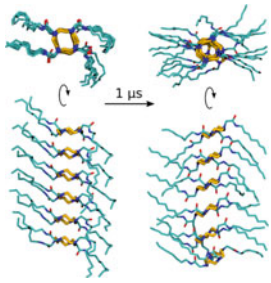

Fig. 2 Snapshots of the 6 DOTA stack at the beginning and at the end of the 1DOTA simulation. Very good conservation of the stacked configuration could be observed even after 1 μs of simulation within the membrane environment. Alkyl tails of DOTA prefer to align in a parallel configuration and also parallel to the membrane plane

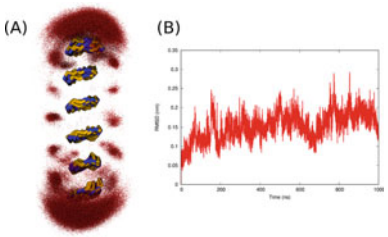

Fig. 3 **A** Water density around the DOTA central ring stack in simulation 1DOTA. Water oxygen atoms were represented as red dots overlaid for multiple frames during simulation. The DOTA stack in each frame was fitted to the starting structure using the nitrogen atoms of the central ring as alignment subset. Water binding sites located in between the -N-H and -C = O groups on both sides of the rings could be identified. Visual inspection of the trajectories revealed jumping events of water molecules between these sites. **B** RMSD of DOTA stack with respect to the starting configuration

3 Molecular Dynamics for Assessing the Formation of Polyplexes

The molecular dynamics (MD) also have found its applicability in ascertaining the formation of polyplexes. The polyplexes are special types of complexes formed between nucleic acids (DNA/RNA) and (macro)molecular entities (*e.g.*, polycations, polyelectrolytes, polypeptides). In the last decades, the polyplexes have received distinct attention due to their potential usage in gene therapy. This therapy implies the insertion of nucleic acids into cells; thereby altering the gene expression aiming to correct gene defects (Anderson 1984). Two main approaches are actually adopted in gene therapy, the first one deal with *viral vectors* for transporting the genetic material (Hawley et al. 1994; Kay et al. 2001; Vannucci et al. 2013), and the second approach uses the cationic non-viral vectors (Li and Huang 2000; Wu and Wu 1987). In the last decade, the focus of the research has started to shift from viral vectors to non-viral vectors. This is because the usage of viruses for gene therapy implies some risks. The main assets of non-viral vectors involve (1) the inferior specific immune reaction, (2) the safer responses, (3) the simpler design, and (4) chemical properties for various purposes (Han et al. 2000; Luo and Saltzman 2000; Mintzer and Simanek 2009; Tang and Szoka 1997). As non-viral vectors, cationic polymers are often employed owing to their capacity to interact readily with nucleic acids by forming polyplexes. The most explored polymers as non-viral vectors deal with linear or branched poly(ethylene imine) (PEI) and polypeptide-type poly(L-Lysine) (PLL) (Mintzer and Simanek 2009; Nicolas et al. 2013). According to previous studies, PLL is more advantageous in comparison to PEI in terms of cytotoxicity (Godbey et al. 1999). This is because PLL is more biodegradable in vivo than PEI. However, PLL demonstrated a lower transfection efficiency if compared to PEI (Tang and Szoka 1997).

Ziebarth and co-workers carried out molecular dynamics simulations of a short DNA duplex d(CGCGAATTCGCG) in the presence of PEI or PLL to reveal the specific interactions in the course of polyplexes formation (Ziebarth and Wang 2009).

In their study, all simulations were carried out using the Amber Parm99 force field and the AMBER-8 software package for the molecular dynamics. After an initial separation of about 50 Å, the DNA and polycation interacted by forming a stable polyplex within 10 ns (ns). The DNA did not undergo any major structural changes on complexation and remained in the B-form. The polyplexes were formed by the interaction of the charged amine groups of polycations and DNA phosphate groups. Thus, polycations were able to intrude into the major and minor grooves of DNA, depending on the identity and the charge state of the polycation. Ultimately, these authors (Ziebarth and Wang 2009) outlined that, in comparison with PLL, PEI was able to neutralize the charge of DNA in a more efficient way.

In another study undertaken by Sun and collaborators (Sun et al. 2011), the molecular dynamics simulation was performed towards understanding the mechanisms of DNA complexation with PEI. These authors investigated the effect of PEI branching and its protonation state. Drew-Dickerson dodecamer was employed as simulated DNA. And, its initial structure was built to be canonical B-form using the AMBER NAB tool. Four molecular structures of PEI were considered with similar molecular mass (570 Da), but different degrees of branching: (1) pure linear chain, (2) semi-linear, (3) moderately branched geometry and (4) hyper-branched structure. These authors employed the NAMD package for MD simulations using the CHARMM-27 force field. Finally, they found that the degree of branching had a smaller influence on the DNA binding than the protonation state of the polymeric vectors. In addition, it was reported that 46% of protonated PEI formed more stable complexes with DNA than the 23% protonated PEI. Likewise, these authors highlighted that PEI interacted with the DNA through the formation of hydrogen bonding with the backbone oxygens. Two types of hydrogen bonding were evidenced, *i.e.* direct hydrogen bonding and indirect hydrogen bonding (mediated through water molecules).

Regarding the flexibility of DNA macromolecule, a seminal MD study was reported evidencing the relative flexibility in aqueous solutions of DNA compared to RNA (Noy et al. 2004). The essential dynamics analysis (of 10 ns trajectories) suggested that the pattern of the flexibility of DNA and RNA duplexes was different. Moreover, MD simulations (performed by means of AMBER6·1 program) demonstrated that the concepts of flexibility, stiffness, and deformability are much complex. For instance, the DNA duplex can be more flexible for some perturbations and more rigid for others (Noy et al. 2004). Another study dealt with molecular dynamics (assuming the OPLS-AA force field) to approximate localization of structural water molecules in DNA (Neder et al. 2005). Thus, these authors unveiled by MD simulation the first hydration shell of double-helix DNA in the A- and B-conformations. It is worth noting that the MD simulations were also employed for assessing DNA-protein and DNA-drug interactions, detailing the dynamics, and stability of such types of complexes (Lei et al. 2012; MacKerell Jr and Nilsson 2001).

Our group started to approach the subject of the formation of the polyplexes back from 2015. For example, in reference (Clima et al. 2015) it was reported the experimental design, modeling, and optimization of the polyplex formation between double-stranded oligonucleotides (dsDNA) and branched poly(ethylene imine) (b-PEI). A design of experiments was adopted to investigate experimentally the binding

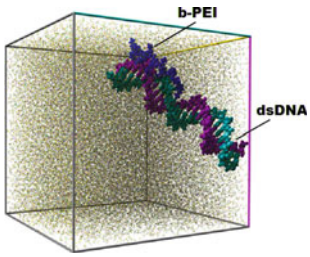

Fig. 4 Rendering of the dsDNA/b-PEI polyplex resulted from MD simulation (at $t = 21$ ns) in a simulation box with explicit water molecules (solvent) (Clima et al., 2015)

efficiency of DNA and branched-PEI under various conditions. Moreover, the molecular dynamics simulation was performed to disclose the mechanism of polyplex formation at the atomic-scale. In this work, the dsDNA composed of 50 nucleotides was exploited in modeling study and experimental validation. Thus, the sense strand of dsDNA was 5′- CAAGCCCTTAACGAACTTCAACGTA-3′, and correspondingly, the antisense strand was 5′-TACGTTGAAGTTCGTTAAGGGCTTG-3′. The molecular dynamics simulations were carried out by means of the YASARA-Structure software package (Krieger et al. 2014), which is an all-in-one program for molecular modeling. In fact, YASARA is a molecular-graphics, -modeling and -simulation program with an intuitive user interface and photorealistic graphics (Krieger and Vriend 2014). It contains all AMBER force fields as well as its own force fields (like NOVA, YASARA, and YAMBER). Note that, the YASARA-Structure program includes an automatic parameterization method ('AutoSMILES'), which is very facile to get the molecular mechanics parameters for the unknown structures. According to the report of the developers (Krieger and Vriend 2014), the YASARA program has been developed to boost molecular dynamics simulations in the frame of the all-in-one program environment. In the published study (Clima et al. 2015), the molecular dynamics simulation was done at the level of the YASARA force field, which includes the self-parameterizing knowledge-based potentials. Hence, the resulted DNA/PEI polyplex (at 21 ns simulation time) in an explicit solvent (water model TIP3P) is illustrated in Fig. 4.

Finally, the results of the simulation disclosed that hydrogen atoms from b-PEI amine groups mainly interacted with oxygen atoms from dsDNA phosphate groups. These interactions conducted to the formation of hydrogen bonds between dsDNA and b-PEI macromolecules; thereby stabilizing the polyplex structure. As regards the polyplex conformation, the polycation chain remained close to the DNA making contacts in the vicinity of a minor groove site (Clima et al. 2015).

A continuation of studies dealing with polyplexes (Dascalu et al. 2017; Vasiliu et al. 2018; Vasiliu et al. 2017) has been performed in the frame of ERA Chair SupraChemLab project implemented at the Centre of Advanced Research in Bionanoconjugates and Biopolymers at ICMPP from Iasi, Romania. For instance, the optimization of polyplex formation between dsDNA and poly(L-Lysine) (PLL) has been reported in reference (Vasiliu et al. 2017). Here, the MD simulations were performed at the level of the YASARA force filed to reveal the formation of dsDNA-PLL polyplexes at different solution pH, and consequently at different protonation degree of PLL (see Fig. 5).

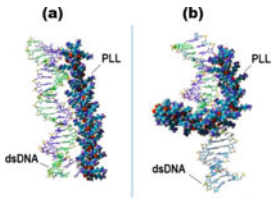

Fig. 5 Rendering of the dsDNA/PLL polyplex indicated by MD simulation (at t = 35 ns), (a) pH 5·4 (100% protonation of PLL), (b) pH 7·4 (50% protonation of PLL); explicit water molecules omitted for clarity (Vasiliu et al., 2017)

Thus, MD results disclosed that the binding rate between macromolecules was changed with the variation of PLL protonation. More detailed, at pH 5·4 (*i.e.*, 100% PLL protonation), the distance between dsDNA and PLL decreased from 40 Å to 18 Å in just a few nanoseconds of simulation. Instead, at pH 7·4 (*i.e.*, 50% PLL protonation), the same effect was achieved only after 31 ns. Moreover, MD simulation outcomes suggested that hydrogen bonds were mainly formed between the backbone oxygen atoms of dsDNA and hydrogen atoms of amine groups from PLL. Likewise, computational data showed that the PLL was the most flexible macromolecule, which could be bent and twisted to a greater extent at physiological pH value. In contrast, the dsDNA conformation in polyplex was minimally perturbed during MD simulations. It should be specified here that the formation of the dsDNA-PLL polyplex was validated experimentally using gel electrophoresis assays. The optimal conditions of complexation (pH 5·4 and N/P ratio of 125) were established by means of the response surface methodology (Vasiliu et al. 2017). Likewise, it should be noticed that the binding interaction between dsDNA and PLL was proved also by other authors using different experimental techniques such as fluorescamine assay (Read et al. 1999) and time-resolved multi-angle laser light scattering (Lai and van Zanten 2001).

In another study (Vasiliu et al. 2018) it was shown (by MD simulations in YASARA) the possibility of the polyplex formation between a cyclodextrin-based vector and two oligomeric chains of dsDNA. The non-viral vector represented a polycationic-conjugate assembly comprising beta-cyclodextrin (β-CD) as a core that was grafted with one chain of poly(ethylene glycol) (PEG) and six branches of PEI. The conjugated vector/carrier was denoted as (β-CD-PEG-PEI). The molecular dynamics trajectories revealed that the polycationic conjugate (β-CD-PEG-PEI) was flexible and interacted very fast with both dsDNA macromolecules (Vasiliu et al. 2018). For example, at simulation time $t = 2{\cdot}5$ ns, five of PEI branches interacted evidently with the nucleotides from both dsDNA helixes (Fig. 6). This computational study was also supported by the Gel Red staining assay for experimental validation of the polyplex formation (Vasiliu et al. 2018).

More advanced studies were also performed to shed light on the supramolecular interactions between several molecules of the conjugate (β-CD-PEG-PEI) and a longer chain of dsDNA helix (Dascalu et al. 2017). In this respect, the molecular modeling, dynamics simulations, and trajectories analysis were carried out using the high-performing software packages like YASARA (Krieger and Vriend 2014),

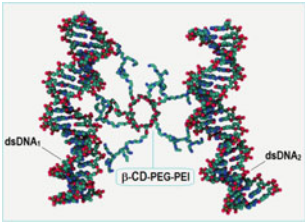

Fig. 6 Rendering of the polyplex supramolecular structure derived from MD simulation (at t = 2·5 ns) showing the interaction between the polycationic conjugate vector (β-CD-PEG-PEI) and two macromolecules of dsDNA; explicit water molecules omitted for clarity (Vasiliu et al., 2018)

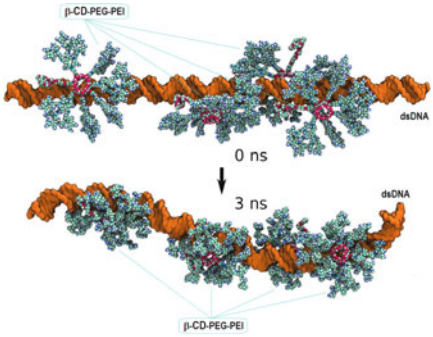

Fig. 7 Rendering of the polyplex supramolecular conformation resulted from MD simulation showing the bending of the dsDNA chain (96 bp long) in the presence of four polycationic vectors (β-CD-PEG-PEI); explicit water molecules omitted for clarity (Dascalu et al., 2017)

Maestro simulation environment, GROMACS (Abraham et al. 2015), and VMD (Humphrey et al. 1996). In one of the simulations, four entities of β-CD-PEG-PEI conjugate vector were placed in the vicinity of a dsDNA helix (96 base-pairs long), in a "face-on" orientation as starting conformation. After 3 ns of MD simulation, the dsDNA fragment started to bend (Fig. 7). And, the four vectors (β-CD-PEG-PEI) revealed a conformational adaptation to dsDNA surface as a consequence of maximization of the number of *anionic-cationic contacts (i.e.* electrostatic interactions*).* The more advanced *in silico* molecular modeling performed in this study (Dascalu et al. 2017) suggested that the developed non-viral vector (β-CD-PEG-PEI) can mimic to some extent the function of histones.

In another report (Uritu et al. 2015), a siloxane-based conjugate carrier was assessed as a non-viral vector for the polyplex formation. This vector (denoted as cD_4^H-AGE-PEI) comprised a cyclic siloxane ring (2,4,6,8-tetramethylcyclotetrasiloxane, cD_4^H) as a core that was conjugated with polyethyleneimine (PEI) chains as cationic branches. The MD simulations (performed at the level of the YASARA force field) disclosed the interaction of the cD_4^H-AGE-PEI with the Drew-Dickerson dodecamer $d(CGCGAATTCGCG)_2$. The MD simulation results proved the interaction between cD_4^H-AGE-PEI and dsDNA with the formation of hydrogen bonds that stabilized the polyplex conformation (Fig. 8).

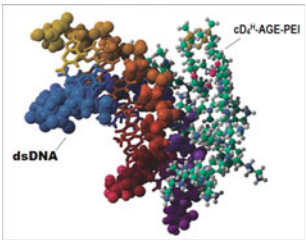

Fig. 8 Rendering of the polyplex structure resulted from MD simulation ($t = 2$ ns), showing the interaction between the non-viral vector (cD_4^H-AGE-PEI) and dsDNA helix; explicit water molecules omitted for clarity (Uritu et al., 2015)

4 Molecular Dynamics Simulation to Estimate Solute-Solvent Interactions

The molecular dynamics (MD) simulation can be employed in the exploration of the solute-solvent interactions by providing dynamic pictures and valuable insights of such complex systems (Zhao et al. 2013). In this respect, the reference (Airinei et al. 2017) reported the solvatochromic analysis and computational study of the *azobenzene maleimide compound* (AMC). It should be mentioned that *azobenzene derivatives* are molecular entities of real interest. These molecules are able to provide a response to external stimuli, which allow the control of their photophysical properties (Cojocaru et al. 2013). Owing to their particular trans/cis isomerization reaction (Isac et al. 2019), the azobenzene derivatives have found the applicability in various fields such as photoresponsive materials, optical data storage, liquid crystal displays, and others (Cojocaru et al. 2013; Isac et al. 2019).

In the reference (Airinei et al. 2017), the molecular dynamics (MD) simulations were carried out to detail the solvation of azobenzene maleimide molecule in two polar solvents (acetone and ethylene glycol). Both solvents were modeled as explicit molecules surrounding the solute. Hence, short-term MD simulations were done using the YASARA force-field. Results of the MD simulation highlighting the solute-solvent interactions are illustrated in Fig. 9.

Simulation outcomes suggested the formation of hydrogen bonds (H-bonds) between the solute (AMC – *azobenzene maleimide compound*) and both polar

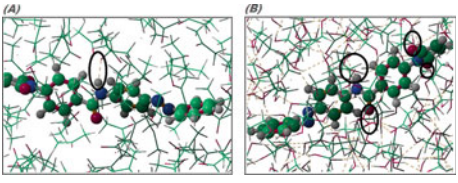

Fig. 9 Rendering of the solute-solvent systems showing the interactions of the solute molecule (*azobenzene maleimide*) with explicit solvents: (*A*) acetone and (*B*) ethylene glycol; equilibrated solute-solvent systems after energy minimization and short molecular dynamics (10 ps); computations were done using the YASARA force field

solvents. These H-bonds are represented as dot lines in Fig. 9. The emerged H-bonds, as a consequence of solute-solvent interactions, were encircled in Fig. 9 just for clarity. As one can see from Fig. 9A, the AMC solute formed one hydrogen bond with a molecule of the acetone solvent. Here, the NH group from the amide moiety of AMC acted as hydrogen bond donor (HBD), while the oxygen atom from acetone acted as hydrogen bond acceptor (HBA). The computed distance of the hydrogen bond was equal to 1·94 Å. And, the associated energy was found to be 5·47 kcal/mol.

In the case of ethylene glycol as solvent (Fig. 9B), the calculation results revealed the formation of many hydrogen bonds between solvent molecules in the simulating environment. In addition, the simulation indicated the formation of four H-bonds between the solute (*azobenzene maleimide*) and solvent (ethylene glycol) (see Fig. 9B). Thus, the carbonyl groups from amide and maleimide moieties of AMC acted as proton acceptors (HBA) yielding the formation of three hydrogen bonds. The fourth H-bond appeared between amide NH of the solute (HBD) and the oxygen atom (HBA) from ethylene glycol molecule (Fig. 9B). The calculated distances of these hydrogen bonds ranged from 1·71 Å to 1·85 Å. And, the total hydrogen bond energy was equal to 22·23 kcal/mol for the system *azobenzene maleimide/ethylene glycol*.

A more detailed computational chemistry study of azobenzene maleimide compounds was given in the reference (Isac et al. 2019). These computations were done to explore the electronic structures and to reveal the charge-transfer excitation effects at the level of the density functional theory (DFT) (Isac et al. 2019). Likewise, the solute-solvent interactions were assessed by computational chemistry methods and for other organic molecules, such as pyrazoline derivative compounds (Chibac et al. 2019).

5 Conclusions

In the course of implementation of the SupraChemLab project within the H2020 Call, we have investigated by means of molecular dynamics the formation and evolutions of different supra-molecular assemblies and systems. The computer-aided simulations by molecular dynamics have contributed considerably to understanding of the investigated structures and phenomena. Thus, MD simulations revealed the stability of DOTA self-assembly aggregate in the phospholipid (POPC) membrane and its functionality as the artificial channel for water permeation. Dynamic simulations disclosed also important insights regarding the stability of the studied polyplexes formed as the supra-molecular assemblies between dsDNA and non-viral vectors. Likewise, the MD method can be applied to evaluate the solute-solvent interactions.

Acknowledgements The project leading to this application has received funding from the H2020 ERA Chairs Project no 667387: SupraChem Lab Laboratory of Supramolecular Chemistry for Adaptive Delivery Systems ERA Chair initiative.

Conflict of interest The authors declare no conflict of interest.

References

Abraham MJ, Murtola T, Schulz R, Páll S, Smith JC, Hess B, Lindahl E (2015) GROMACS: high performance molecular simulations through multi-level parallelism from laptops to supercomputers. SoftwareX 1–2:19–25. https://doi.org/10.1016/j.softx.2015.06.001

Airinei A, Isac DL, Homocianu M, Cojocaru C, Hulubei C (2017) Solvatochromic analysis and DFT computational study of an azomaleimide derivative. J Mol Liq 240:476–485. https://doi.org/10.1016/j.molliq.2017.05.096

Anderson WF (1984) Prospects for human gene therapy. Science 226(4673):401–409

Barboiu M (2016) Artificial water channels–incipient innovative developments. Chem Commun 52(33):5657–5665

Becker OM, Watanabe M (2001) Dynamics methods. In: Becker OM, MacKerell Jr AD, Roux B, Watanabe M, Marcel Dekker (eds) Computational biochemistry and biophysics. New York, pp 39–67

Chibac AL, Roman G, Cojocaru C, Shova S, Sacarescu G, Simionescu M, Sacarescu L (2019) Bichromophoric pyrazoline derivative with solvent-selective photoluminescence quenching. J Mol Liq 278:156–163. https://doi.org/10.1016/j.molliq.2019.01.067

Clima L, Ursu EL, Cojocaru C, Rotaru A, Barboiu M, Pinteala M (2015) Experimental design, modeling and optimization of polyplex formation between DNA oligonucleotides and branched polyethylenimine. Org Biomol Chem 13(36):9445–9456

Cojocaru C, Airinei A, Fifere N (2013) Molecular structure and modeling studies of azobenzene derivatives containing maleimide groups. SpringerPlus 2(1):586. https://doi.org/10.1186/2193-1801-2-586

Dascalu A, Ardeleanu R, Neamtu A, Maier S, Uritu C, Nicolescu A, Silion M, Peptanariu D, Calin M, Pinteala M (2017) Transfection-capable polycationic nanovectors which include PEGylated-cyclodextrin structural units: a new synthesis pathway. J Mater Chem B 5(34):7164–7174

Godbey W, Wu KK, Mikos AG (1999) Tracking the intracellular path of poly (ethylenimine)/DNA complexes for gene delivery. Proc Natl Acad Sci 96(9):5177–5181

Guvench O, MacKerell AD (2008) Comparison of protein force fields for molecular dynamics simulations. In: Kukol A (eds) Molecular modeling of proteins. methods molecular biology, vol 443. Humana Press/Springer, pp 63–88. https://doi.org/10.1007/978-1-59745-177-2_4

Han S-O, Mahato RI, Sung YK, Kim SW (2000) Development of biomaterials for gene therapy. Mol Ther 2(4):302–317

Hawley R, Lieu F, Fong A, Hawley TS (1994) Versatile retroviral vectors for potential use in gene therapy. Gene Ther 1(2):136

Humphrey W, Dalke A, Schulten K (1996) VMD: visual molecular dynamics. J Mol Graph 14(1):33–38. https://doi.org/10.1016/0263-7855(96)00018-5

Isac DL, Airinei A, Maftei D, Humelnicu I, Mocci F, Laaksonen A, Pinteală M (2019) On the charge-transfer excitations in Azobenzene Maleimide compounds: a theoretical study. J Phys Chem A 123(26):5525–5536. https://doi.org/10.1021/acs.jpca.9b02082

Jensen F (2007) Introduction to computational chemistry, 2nd edn. Wiley, Chichester, pp 22–77

Kay MA, Glorioso JC, Naldini L (2001) Viral vectors for gene therapy: the art of turning infectious agents into vehicles of therapeutics. Nat Med 7(1):33–40

Khalili-Araghi F, Gumbart J, Wen P-C, Sotomayor M, Tajkhorshid E, Schulten K (2009) Molecular dynamics simulations of membrane channels and transporters. Curr Opin Struct Biol 19(2):128–137

Krieger E, Koraimann G, Vriend G (2002) Increasing the precision of comparative models with YASARA NOVA—a self-parameterizing force field. Proteins Struct Function Bioinform 47(3):393–402

Krieger E, Vriend G (2014) YASARA View—molecular graphics for all devices—from smartphones to workstations. Bioinformatics 30(20):2981–2982

Krieger E, Vriend G (2015) New ways to boost molecular dynamics simulations. J Comput Chem 36(13):996–1007

Lai E, van Zanten JH (2001) Monitoring DNA/Poly-l-Lysine polyplex formation with time-resolved multiangle laser light scattering. Biophys J 80(2):864–873. https://doi.org/10.1016/S0006-3495(01)76065-1

Lei H, Wang X, Wu C (2012) Early stage intercalation of doxorubicin to DNA fragments observed in molecular dynamics binding simulations. J Mol Graph Model 38:279–289

Lewars E (2004) Computational chemistry. Introduction to the theory and applications of molecular and quantum mechanics. Kluwer Academic Publishers, pp 43–79

Li S-D, Huang L-Y (2000) Nonviral gene therapy: promises and challenges. Gene Ther 7(1):31–34

Luo D, Saltzman WM (2000) Synthetic DNA delivery systems. Nat Biotechnol 18(1):33–37

MacKerell Jr AD (2001) Atomistic models and force fileds. In: Becker OM, MacKerell Jr AD, Roux B, Watanabe M (eds) Computational biochemistry and biophysics. Marcel Dekker, New York pp 7–38

MacKerell Jr AD, Nilsson L (2001) Nucleic acid simulations. In: Becker OM, MacKerell Jr AD, Roux B, Watanabe M (eds) Computational biochemistry and biophysics. Marcel Dekker, New York, pp 441–463

Mintzer MA, Simanek EE (2009) Nonviral vectors for gene delivery. Chem Rev 109(2):259–302

Murail S, Vasiliu T, Neamtu A, Barboiu M, Sterpone F, Baaden M (2018) Water permeation across artificial I-quartet membrane channels: from structure to disorder. Faraday Discuss 209:125–148

Neder ADVF, de Oliveira Neto M (2005) A simple low-cost simulation protocol for approximate localization of structural water molecules in DNA oligonucleotides. J Braz Chem Soc 16(3B):597–606

Nicolas J, Mura S, Brambilla D, Mackiewicz N, Couvreur P (2013) Design, functionalization strategies and biomedical applications of targeted biodegradable/biocompatible polymer-based nanocarriers for drug delivery. Chem Soc Rev 42(3):1147–1235

Noy A, Perez A, Lankas F, Luque FJ, Orozco M (2004) Relative flexibility of DNA and RNA: a molecular dynamics study. J Mol Biol 343(3):627–638

Read ML, Etrych T, Ulbrich K, Seymour LW (1999) Characterisation of the binding interaction between poly(L-lysine) and DNA using the fluorescamine assay in the preparation of non-viral gene delivery vectors. FEBS Lett 461(1–2):96–100. https://doi.org/10.1016/s0014-5793(99)01435-0

Sun C, Tang T, Uludağ H, Cuervo JE (2011) Molecular dynamics simulations of DNA/PEI complexes: effect of PEI branching and protonation state. Biophys J 100(11):2754–2763

Tang M, Szoka F (1997) The influence of polymer structure on the interactions of cationic polymers with DNA and morphology of the resulting complexes. Gene Ther 4(8):823–832

Uritu CM, Calin M, Maier SS, Cojocaru C, Nicolescu A, Peptanariu D, Constantinescu CA, Stan D, Barboiu M, Pinteala M (2015) Flexible cyclic siloxane core enhances the transfection efficiency of polyethylenimine-based non-viral gene vectors. J Mater Chem B 3(42):8250–8267. https://doi.org/10.1039/C5TB01342A

Vannucci L, Lai M, Chiuppesi F, Ceccherini-Nelli L, Pistello M (2013) Viral vectors: a look back and ahead on gene transfer technology. New Microbiol 36(1):1–22

Vasiliu T, Cojocaru C, Peptanariu D, Dascalu AI, Pinteala M, Rotaru A (2018) Polyplex formation between cyclodextrin-based non-viral vector and dsDNA: molecular dynamic study with experimental validation. Rev Roum Chim 63(7–8):629–636

Vasiliu T, Cojocaru C, Rotaru A, Pricope G, Pinteala M, Clima L (2017) Optimization of polyplex formation between dna oligonucleotide and poly (L-Lysine): experimental study and modeling approach. Int J Mol Sci 18(6):1291

Wu GY, Wu CH (1987) Receptor-mediated in vitro gene transformation by a soluble DNA carrier system. J Biol Chem 262(10):4429–4432

Zhao Y, Liu X, Wang J, Zhang S (2013) Effects of anionic structure on the dissolution of cellulose in ionic liquids revealed by molecular simulation. Carbohyd Polym 94(2):723–730. https://doi.org/10.1016/j.carbpol.2013.02.011

Ziebarth J, Wang Y (2009) Molecular dynamics simulations of DNA-polycation complex formation. Biophys J 97(7):1971–1983